Cross-linking analysis of the ryanodine receptor and α_1-dihydropyridine receptor in rabbit skeletal muscle triads

Brendan E. MURRAY and Kay OHLENDIECK*

Department of Pharmacology, University College Dublin, Belfield, Dublin 4, Ireland

In mature skeletal muscle, excitation–contraction (EC) coupling is thought to be mediated by direct physical interactions between the transverse tubular, voltage-sensing dihydropyridine receptor (DHPR) and the ryanodine receptor (RyR) Ca^{2+} release channel of the sarcoplasmic reticulum (SR). Although previous attempts at demonstrating interactions between purified RyR and α_1-DHPR have failed, the cross-linking analysis shown here indicates low-level complex formation between the SR RyR and the junctional α_1-DHPR. After cross-linking of membranes highly enriched in triads with dithiobis-succinimidyl propionate, distinct complexes of more than 3000 kDa were detected. This agrees with numerous physiological and electron-microscopic findings, as well as co-immunoprecipitation experiments with triad receptors and receptor domain-binding studies. However, a distinct overlap of immunoreactivity between receptors was not observed in crude microsomal preparations, indicating that the triad complex is probably of low abundance. Disulphide-bonded, high-molecular-mass clusters of triadin, the junctional protein proposed to mediate interactions in triads, were confirmed to be linked to the RyR. Calsequestrin and the SR Ca^{2+}-ATPase were not found in cross-linked complexes of the RyR and α_1-DHPR. Thus, whereas recent studies indicate that the two receptors exhibit temporal differences in their developmental inductions and that receptor interactions are not essential for the formation and maintenance of triads, this study supports the signal transduction hypothesis of direct physical interactions between triad receptors in adult skeletal muscle.

INTRODUCTION

Excitation–contraction (EC) coupling, the process by which neuronal-induced depolarization of the surface membrane leads to the release of Ca^{2+} ions from the sarcoplasmic reticulum (SR) and thereby the initiation of skeletal muscle contraction, is mediated at the triad junction [1,2]. These highly specialized peripheral couplings are internal muscle membrane junctions composed of a central transverse tubule and two terminal cisternae of the junctional SR [3]. Although other Ca^{2+} release mechanisms have been proposed, currently the most acceptable model for EC coupling in skeletal muscle assumes direct physical interactions between junctional triad receptors [1,2]. In mature skeletal muscle, direct protein–protein interactions between the voltage-sensing, transverse tubular dihydropyridine receptor (DHPR) and the ryanodine receptor (RyR) Ca^{2+} release channel of the SR are proposed to trigger Ca^{2+} release from the SR lumen [1–3].

The DHPR represents a voltage-dependent L-type channel that exists as a multimeric complex of α_1, α_2/δ, β and γ subunits [4]. Whereas the α_1-subunit was shown to be the principal subunit that carries properties for voltage sensing and ion permeability, other subunits are implemented in the targeting and modulation of channel activity [5]. The RyR consists of four identical 565 kDa subunits [6] and is tightly associated with the 12 kDa FK-506 binding protein that modulates Ca^{2+} channel gating [7]. Cryoelectron microscopy and three-dimensional reconstruction of the high-molecular-mass RyR complex revealed a relatively compact structure and demonstrated that major conformational changes underlie the opening and closing mechanism of the Ca^{2+} channel pore [8].

Numerous physiological studies [9,10] and ultrastructural findings [3,11], as well as binding experiments with receptor domains [12] and differential receptor co-immunoprecipitation [13], support the existence of a triadic linkage between the RyR and the DHPR. Because both classes of skeletal muscle receptor co-localize during normal development [14], molecular interactions between the SR RyR and the transverse tubular DHPR might not only be involved in the maintenance of peripheral membrane couplings but could also be responsible for the initial formation of triad junctions [15]. In cell lines from dysgenic *mdg/mdg* mice, which have a primary defect in the α_1-subunit of the DHPR, targeting of the α_2-DHPR is incorrect and to a large extent the RyR and triadin do not exhibit the characteristic formation of clusters as observed in normal muscle cells [16].

Other junctional membrane components have been proposed to be required for the regulation and stabilization of interactions between the DHPR and the RyR. SR proteins such as calsequestrin, the junctional 90 kDa protein and triadin are implicated in the triadic signal transduction mechanism, Ca^{2+} handling and/or triad architecture [17–20]. Triadin is thought to anchor calsequestrin to the junctional region of the SR and this protein might also be involved in the functional coupling between the RyR and DHPR [17–20]. In addition, other subpopulations of muscle proteins suggested to participate in triad complexes are glyceraldehyde-3-phosphate dehydrogenase [21,22], aldolase [22,23], the Na^+/Ca^{2+}-exchanger and the calmodulin-sensitive Ca^{2+}-ATPase [24].

Despite the above evidence for receptor linkage in skeletal muscle triads, direct molecular interactions between isolated RyR and DHPR were not observed with protein overlay techniques and affinity chromatography [22]. Hence, to provide more

Abbreviations used: BS^3, bis-sulphosuccinimidyl suberate; DSP, dithiobis-succinimidyl propionate; DHPR, dihydropyridine receptor; EC, excitation–contraction; mAb, monoclonal antibody; RyR, ryanodine receptor; SR, sarcoplasmic reticulum.

* To whom correspondence should be addressed.

direct biochemical evidence for the existence of a native triad complex, we performed cross-linking studies of key components of EC coupling by using crude microsomal membranes, enriched triad fractions and heavy SR vesicles. To identify complexed proteins unequivocally, immunoblotting with highly specific antibodies against key components of EC coupling was employed.

MATERIALS AND METHODS

Materials

Protease inhibitors, chemiluminescence Western blotting substrates and peroxidase-conjugated secondary antibodies were purchased from Boehringer Mannheim (Lewis, East Sussex, U.K.). Prestained molecular mass markers were from Bethesda Research Laboratories (Gaithersburg, MD, U.S.A.) and all cross-linkers were obtained from Pierce & Warriner (Chester, Cheshire, U.K.). Immobilon-NC nitrocellulose was obtained from Millipore Corporation (Bedford, MA, U.S.A.). All other chemicals were of analytical grade and purchased from Sigma Chemical Company (Poole, Dorset, U.K.).

Isolation of skeletal muscle membranes

Crude skeletal muscle microsomal membranes were isolated from New Zealand White rabbits by a modification of a method previously described in detail [25]. All preparative steps were performed at 0–4 °C and all buffers contained a protease inhibitor cocktail (1 mM EDTA/0.2 mM Pefabloc/1.4 μM pepstatin A/0.15 μM aprotinin/0.3 μM E-64/1 μM leupeptin/0.5 μM soybean trypsin inhibitor) to minimize protein degradation. Hind leg and back muscles were dissected and homogenized in 7 vol. of buffer A [20 mM Tris/maleate (pH 7.0)/3 mM EGTA/10 % (w/v) sucrose] with an Ultra-Turrax T25 (IKA-Labortechnik, Staufen, Germany). The homogenate was pelleted for 15 min at 13000 ***g*** in a Sorvall RC-5B centrifuge with a GSA rotor (Sorvall, Wilmington, DE, U.S.A.) and the supernatant fraction was subsequently filtered through three layers of cheesecloth. Pellets were discarded and the supernatant was re-centrifuged for 90 min at 23400 ***g***. The resulting pellet constituted the crude microsomal fraction and was resuspended at a protein concentration of 10 mg/ml in buffer A.

Membrane fractions enriched in triad junctions and preparations derived from the SR were prepared from crude skeletal microsomal membranes based on the procedures of Sharp et al. [26] and Rosemblatt et al. [27], by using a simplified sucrose step gradient. Crude microsomal membranes, resuspended in buffer A, were carefully layered on top of a sucrose bilayer consisting of 17 ml of 28 % (w/v) sucrose and 17 ml of 36 % (w/v) sucrose in 25 mM Tris/maleate (pH 7.0)/3 mM EGTA. Sucrose gradients were centrifuged for 90 min at 140000 ***g*** in an SW-28 rotor (Beckman Corporation, Palo Alto, CA, U.S.A.). Although pellets constituted the membrane fraction highly enriched in vesicles derived from the SR, a well-defined band at the 28 %/36 % interface represented the triad fraction. The bands were carefully collected, diluted 4-fold with buffer B [25 mM Tris/maleate (pH 7.0)/3 mM EGTA], and pelleted by centrifugation at 100000 ***g*** for 35 min. Resuspended membrane pellets were immediately used for cross-linking experiments. Protein concentration was determined by the method of Bradford [28] with BSA and purified myofibrillar proteins as standards.

Chemical cross-linking of muscle membranes

A variety of homobifunctional *N*-hydroxysuccinimidyl ester and imidoester cross-linking reagents were used to elucidate possible interactions between muscle membrane proteins [29,30]. Cross-linkers employed differed in their solubilities and susceptibilities to thiol reagent cleavage, as well as in cross-linker arm length. All stock solutions of cross-linker reagents were solubilized to a concentration of 5 mg/ml. The membrane-permeable reagents [dithiobis-succinimidyl propionate (DSP), dithiobis-sulphosuccinimidyl propionate and dimethyl pimelimidate] were dissolved in DMSO, whereas the water-soluble analogues [disulphosuccinimidyl tartrate and bis-sulphosuccinimidyl suberate (BS^3)] were dissolved in 20 mM citrate, pH 5.0, to minimize hydrolysis in an aqueous environment before the cross-linking assay. The final concentration of DMSO in samples did not exceed 4 % (v/v). Skeletal muscle membrane fractions were diluted with reaction buffer (50 mM Hepes, pH 8.0) to a protein concentration of 2 mg/ml. Cross-linking was performed at room temperature in 50 mM Hepes, pH 8.0, for 30 min with 12.5–100 μg of cross-linker/mg of protein. The reactions were stopped by the addition of 50 μl of 1 M ammonium acetate/ml of reaction mixture. An equal volume of SDS sample buffer [31] was added and the solution was warmed to 37 °C for 10 min before being subjected to electrophoretic analysis.

Gel electrophoresis and densitometric analysis

SDS/PAGE was performed by the method of Laemmli [31] with large 3–12 % and 4–12 % (both w/v) gradient gels, as well as minigels of 5 % and 6 % uniform concentration. For running gels 1.5 mm thick, a Bio-Rad Protean II xi cell 20 cm long was used and for 0.75 mm-thick minigels a Bio-Rad Mini-Protean II electrophoresis system was employed (Bio-Rad Laboratories, Hemel Hempstead, Herts., U.K.). For re-electrophoresis, gel bands were excised and incubated in reducing sample buffer [31] for 15 min and then embedded in 1 % (w/v) agarose on top of SDS/PAGE slab gels. Protein samples were mixed with an equal volume of double-strength sample buffer containing 8 M urea, 2 M thiourea, 3 % (w/v) SDS, 0.05 % Bromophenol Blue and 50 mM Tris/HCl, pH 6.8 (with or without 75 mM dithiothreitol). Each well was loaded with 60 μg of protein; protein bands were revealed by silver staining [32], as well as by Coomassie Blue (G-250) and Stains-all staining [33]. Myofibrils, prepared from rat skeletal muscle homogenates by the method of Etlinger et al. [34], served as a convenient source for high-molecular-mass components including C-protein (140 kDa), M-protein (165 kDa), myomesin (185 kDa), myosin (205 kDa), nebulin (605 kDa) and titin (T1; 2800–3000 kDa). Densitometric scanning of Coomassie Blue-stained gels or silver-stained gels was performed on a Molecular Dynamics 300S computing densitometer (Sunnyvale, CA, U.S.A.) with ImageQuant V3.0 software.

Antibodies to EC-coupling proteins

For the production of sequence-specific polyclonal antisera to the RyR and triadin, as well as the β and γ subunits of the DHPR, peptides representing the last 15 residues of the C-termini of these muscle membrane proteins were coupled to KLH carrier protein by Research Genetics (Huntington, AL, U.S.A.). Antisera were raised by four monthly injections, with the use of standard immunization protocols [35].

Monoclonal antibodies (mAbs) used in this study were a gift from Dr. K. P. Campbell (Howard Hughes Medical Institute, University of Iowa, Iowa City, IA, U.S.A.). mAb IIH11 against the fast-twitch isoform SERCA1 of the SR Ca^{2+}-ATPase, mAb $VIIID1_2$ against calsequestrin, mAbs IIID5 and IIC12 against the α_1-subunit of the DHPR, and mAb IIG12 against triadin

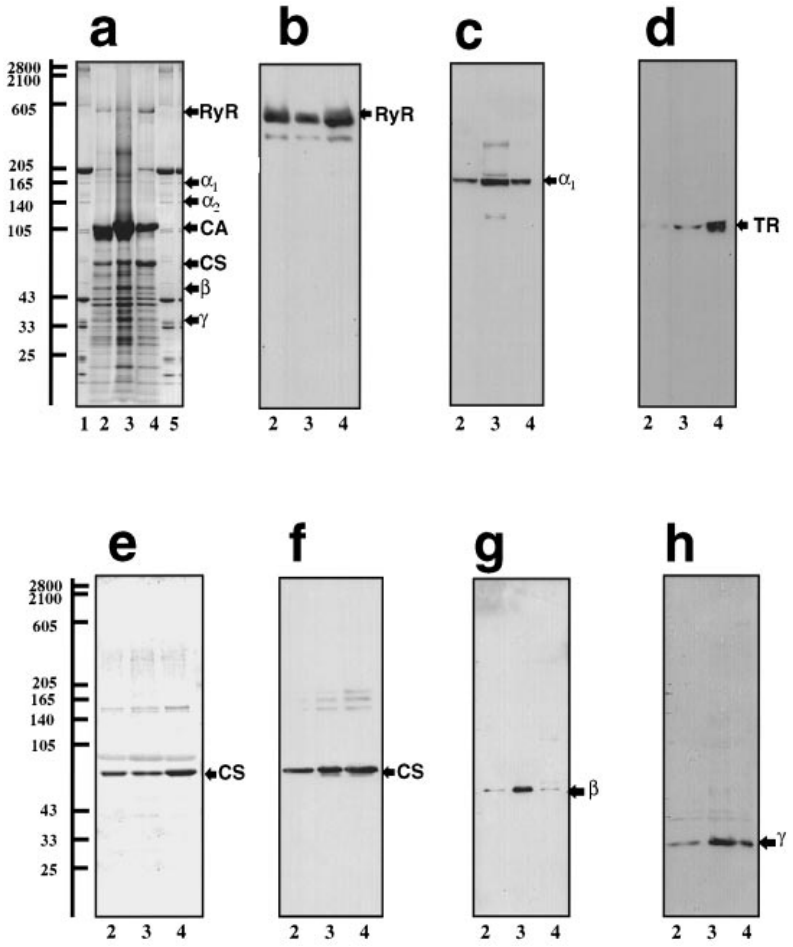

Figure 1 Subcellular fractionation of key components of EC coupling from adult rabbit skeletal muscle

Shown are 4–12% (w/v) gradient gels run under reducing conditions and stained with Coomassie Blue (**a**) and Stains-all (**e**), and identical immunoblots (**b**–**d**, **f**–**h**) of rabbit skeletal muscle microsomes (lanes 2), triads (lanes 3) and the SR (lanes 4). Immunodecoration was performed with polyclonal antibodies against the C-termini of the RyR (**b**) and the β (**g**) and γ (**h**) subunit of the DHPR, as well as mAb IIID5 against α_1-DHPR (α_1) (**c**), mAb IIG12 against triadin (TR) (**d**) and mAb VIIID1$_2$ against calsequestrin (CS) (**f**). Whereas the major bands in the Stains-all-stained gel represent calsequestrin (**e**), the position of the SR Ca^{2+}-ATPase (CA) and the α_2 subunit of the DHPR (α_2) are indicated on the protein gel (**a**). The sizes of molecular mass standards (in kDa), as deduced from rat myofibril marker proteins (**a**, lanes 1 and 5), are indicated at the left.

were produced and characterized as previously described in detail [25].

Affinity purification of monospecific polyclonal antibodies

Monospecific antibodies were purified from crude antisera on the basis of the method by Olmsted [36]. Nitrocellulose strips containing the protein of interest were excised and blocked in 5% (w/v) fat-free milk in 50 mM sodium phosphate (pH 7.4)/0.15 M NaCl (Blotto). After two washes in PBS, the membrane strips were incubated overnight at 4 °C in crude antisera containing 0.5% BSA, 1% (v/v) Tween-20 and 0.02 mM sodium azide. On the next day the membrane strips were washed four times for 10 min each in Blotto, followed by two further washes in PBS. Elution of the bound antibody was achieved by the addition of 100 mM glycine, pH 2.5, for 10 min. The eluted material was then neutralized with unbuffered Tris base to a final pH of 8.0. The eluent was diluted 1:30 with Blotto and used as a source of primary antibody.

Immunoblot analysis

Proteins separated by SDS/PAGE were transferred to nitrocellulose membranes by the method of Towbin et al. [37]. Transfer sheets were blocked for 2 h in Blotto and were then incubated for 3 h with primary antibodies diluted 1:1000. Subsequently, immunoblots were washed twice for 10 min each with 100 ml of Blotto per blot and incubated for 1 h with peroxidase-conjugated secondary antibody at a dilution of 1:1500. After the blots had been washed with Blotto and rinsed with PBS, nitrocellulose sheets were developed by enhanced chemiluminescence. Densitometric scanning of enhanced chemiluminescence blots was performed on a Molecular Dynamics 300S computing densitometer (Sunnyvale, CA, U.S.A.) with ImageQuant V3.0 software.

For reprobing of immunoblots, nitrocellulose sheets were stripped of bound primary and secondary antibody by incubation at 50 °C in 10 mM Tris/HCl (pH 8.0)/0.15 M NaCl/0.1% (v/v) Tween-20/2% (w/v) SDS/100 mM 2-mercaptoethanol for 30 min with gentle shaking. Membranes were then washed twice

in PBS and blocked in Blotto for 1 h before re-probing as outlined above.

RESULTS

To investigate potential interactions between key components of EC coupling, we performed immunoblotting of cross-linked rabbit skeletal muscle membranes. Because EC coupling is mediated at the triad junction, chemical cross-linking of crude microsomes (see Figures 2 and 3), as well as native membrane fractions highly enriched in junctional couplings (see Figures 4 and 5) and the SR (see Figure 6), was employed. For the identification of membrane proteins in cross-linked complexes, a library of established mAbs and novel sequence-specific antibodies to components of EC coupling was used. Silver-stained or Coomassie Blue-stained protein gels, identical in their compositions with the nitrocellulose sheets used in immunoblotting, are shown for comparative purposes.

Immunoblot analysis of key components of EC coupling

Before immunoblotting, the specificity of antibodies for the RyR, calsequestrin, triadin and the α_1, β and γ subunits of the DHPR was tested. As illustrated in Figure 1, subcellular fractionation of skeletal muscle microsomes revealed an enrichment of triadin and calsequestrin in the SR fraction (Figures 1d–1f). The RyR is likewise of high abundance in the SR, but considerable amounts were also found in membranes derived from triad junctions (Figure 1b). In contrast, the α_1-DHPR, and especially the β and γ subunits of this protein complex, are of higher abundance in the transverse-tubule fraction than in the SR (Figures 1c, 1g and 1h). On the basis of these findings we initially investigated microsomes (see Figures 2 and 3) followed by the analysis of triads for potential receptor interactions (see Figures 4 and 5) and the SR for triadin (see Figure 6).

Cross-linking of RyR in skeletal muscle microsomes

Considering that a tetramer of 565 kDa subunits is the established protein complex responsible for Ca^{2+} release from the SR [6], the focus of this investigation was on potential interactions between this Ca^{2+} channel and other proteins proposed to be involved in EC coupling. Increasing amounts of the hydrophobic 1.2 nm cross-linker DSP caused substantial changes in the protein profile of skeletal muscle microsomes (Figure 2a). Because pH 8.0 seemed to give better cross-linking results than pH 7.5 (Figure 2b), optimum conditions at pH 8 were chosen for all subsequent cross-linking experiments. Whereas a relatively comparable protein band pattern was observed for low-molecular-mass proteins, a shift to higher-molecular-mass complexes was seen for proteins greater than apparent 100 kDa (Figure 2a). Immunoblot analysis revealed a considerable decrease in the electrophoretic mobility of the RyR (Figure 2b). A shift from 565 kDa monomers to an extremely high-molecular-mass complex, probably representing a heterogeneous complex including RyR tetramers, was also observed with BS^3 (results not shown). In contrast, incubation of microsomes with disulphosuccinimidyl tartrate, dimethyl pimelimidate and dithiobis-sulphosuccinimidyl propionate resulted in little or no cross-linking of the RyR (results not shown). An exact measurement of the relative molecular mass of the DSP-cross-linked RyR complex was hampered by the non-linear relationship of electrophoretic mobility and very high molecular masses in SDS/PAGE. However, comparison with nebulin and titin isoforms (Figure 1a) suggested an apparent molecular mass of 3–4 MDa.

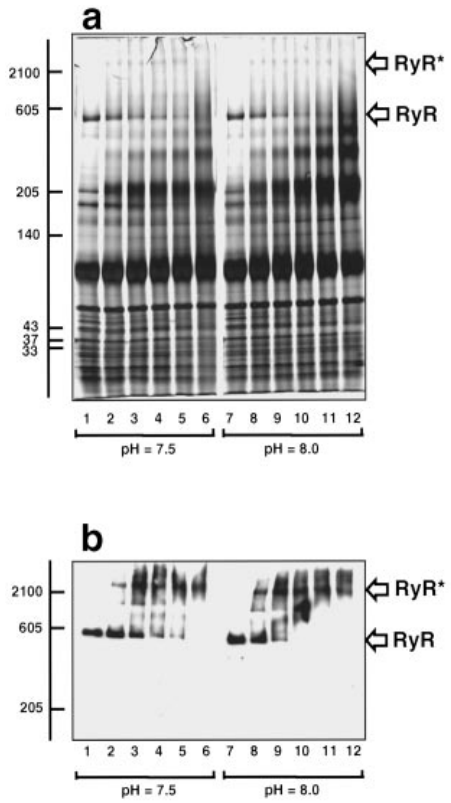

Figure 2 Cross-linking of SR RyR with DSP

Shown are a silver-stained 3–12% (w/v) gradient gel run under non-reducing conditions (**a**) and an identical immunoblot (**b**) of rabbit skeletal muscle microsomes cross-linked with DSP at pH 7.5 (lanes 1–6) and at pH 8 (lanes 7–12). Lanes 1–6 and 7–12 represent 0, 12.5, 25, 37.5, 50 and 100 μg of cross-linker/mg of protein respectively. Immunoblots were decorated with a polyclonal antibody against the C-terminus of the RyR (**b**). Receptor monomers (RyR) and cross-linked high-molecular-mass complexes (RyR*) are marked by open arrows. The positions of molecular mass standards (in kDa) are indicated at the left.

Cross-linking of key components of EC coupling in microsomes

Because DSP resulted in distinct shifts in the relative molecular mass of the RyR (Figure 2b), immunoblot analysis of cross-linked microsomes was also performed with respect to other components involved in EC coupling. As illustrated in Figure 3, DSP caused a decrease in the electrophoretic mobility of α_1-DHPR, β-DHPR, γ-DHPR and calsequestrin. However, the high-molecular-mass complexes of these proteins (Figures 3b–3d and 3f) did not show distinct overlaps of immunoreactivity with the DSP-cross-linked RyR complex (Figure 2b). The smaller DHPR subunits did not shift to the molecular mass range of the α_1-DHPR monomer (Figures 3b–3d). Interestingly, Stains-all staining did not reveal the high-molecular-mass forms of calsequestrin, as was demonstrated by immunoblotting with mAb $VIIID1_2$ (Figures 3e and 3f). Thus staining with the cationic carbocyanine dye is substantially less sensitive than antibody binding with respect to detecting DSP-cross-linked complexes of this SR Ca^{2+}-binding protein.

In control blots, the SR Ca^{2+}-ATPase exhibited distinct cross-linking to higher-molecular-mass complexes estimated to be dimers and tetramers of apparent 110 kDa subunits (Figure 3g). Immunodecoration of triadin under non-reducing conditions before cross-linking was too weak to detect clusters of this protein. However, after cross-linking with DSP, very-high-

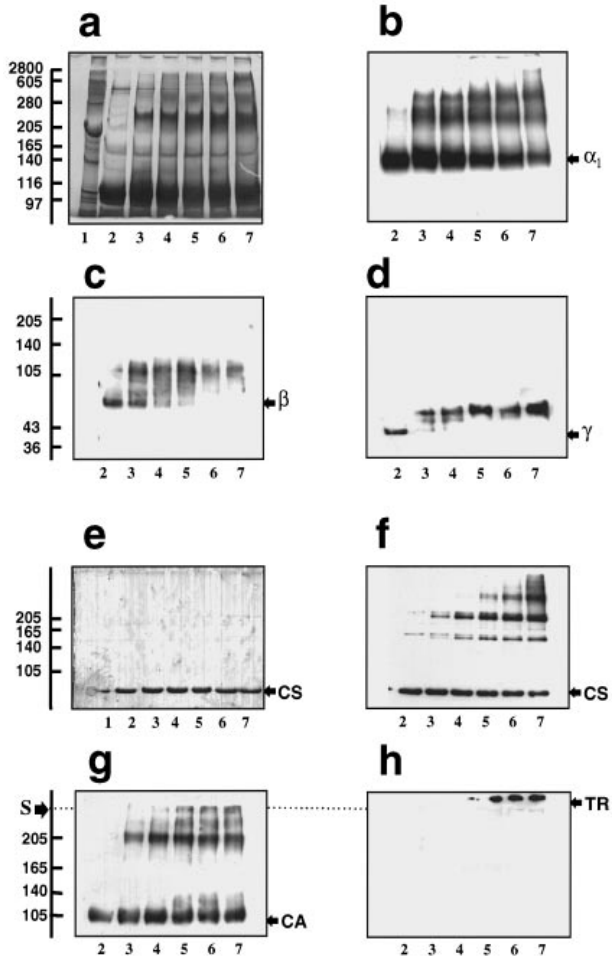

Figure 3 Cross-linking of key components of EC coupling in microsomes by using DSP

Shown are 6% (w/v) minigels run under non-reducing conditions and stained with Coomassie Blue (**a**) and Stains-all (**e**), as well as identical immunoblots (**b**–**d**, **f**–**h**) of rabbit skeletal muscle microsomes cross-linked with DSP. Lanes 2–7 represent 0, 12.5, 25, 37.5, 50 and 100 μg of cross-linker/mg of protein respectively. Immunodecoration was performed with polyclonal antibodies against the C-termini of the β (**c**) and γ (**d**) subunit of the DHPR, as well as mAb IIID5 against α_1-DHPR (**b**), VIIID1$_2$ against calsequestrin (CS) (**f**), mAb IIH11 against the SERCA1 isoform of the SR Ca^{2+}-ATPase (CA) (**g**) and mAb IIG12 against triadin (TR) (**h**). In (**g**) and (**h**) the boundary between the stacking gel and the resolving gel is marked 'S'. The sizes of molecular mass standards (in kDa), as deduced from rat myofibril marker proteins (**a**, lane 1) are indicated at the left.

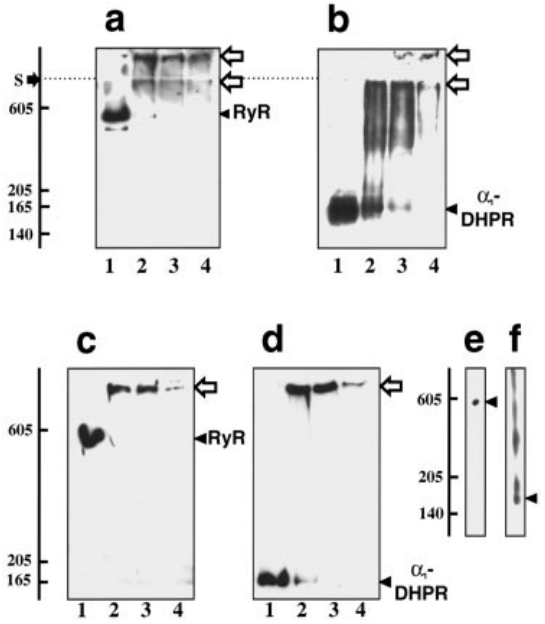

Figure 4 Cross-linking of α_1-DHPR and RyR in triads with DSP

Shown are immunoblots of DSP-cross-linked triads from rabbit skeletal muscle stained with a polyclonal antibody against the C-terminus of the RyR (**a**, **c**, **e**) and mAb IIID5 against the α_1 subunit of the DHPR (**b**, **d**, **f**). For the analysis of complex formation between the α_1-DHPR and the RyR, electrophoretic separation was performed for 440 V h on 6% (w/v) resolving minigels with a stacking gel system (**a**, **b**) and 5% (w/v) resolving minigels without a stacking gel system (**c**, **d**). Distinct overlaps of immunoreactivity for α_1-DHPR and RyR are indicated by large open arrows. Lanes 1–4 represent 0, 25, 50 and 100 μg of cross-linker/mg of protein respectively. In (**e**) and (**f**) are shown immunoblots of samples subjected again to electrophoresis, which were excised from the cross-linked receptor complex and then separated electrophoretically on 6% (w/v) minigels after chemical reduction. Arrowheads indicate the receptor monomers. The boundary between the stacking gel and the resolving gel in (**a**) and (**b**) is marked 'S'. The positions of molecular mass standards (in kDa) are indicated at the left.

molecular-mass complexes were identified in the stacking gel (Figure 3h). In microsomes these distinct triadin complexes did not exhibit an overlap in immunoreactivity with any of the other EC-coupling proteins investigated (results not shown).

Molecular interactions between RyR and α_1-dihydro-pyridine receptor

After the analysis of the effect of cross-linkers on the RyR in microsomes and the finding that crude membranes are not enriched enough in junctional couplings to determine properly the potential interactions with other proteins, the triad fraction of rabbit skeletal muscle was analysed. With the use of non-reducing gels after DSP cross-linking and reducing gels after BS^3 cross-linking, most triad proteins investigated exhibited changes in electrophoretic mobility. However, distinct overlapping immunoreactivity between the RyR complex and other muscle proteins was observed only for the α_1-subunit of the DHPR (Figures 4a–4d). Staining of blots with mAb IIC12 against the α_1-DHPR (results not shown) exhibited the same immunodecorated bands as shown in Figures 4(b) and 4(d) for mAb IIID5. In conventional gels, overlapping immunoreactive bands of the RyR and α_1-DHPR were mainly observed in the stacking gel at a ratio of 50–100 μg DSP/mg of protein (Figures 4a and 4b). To evaluate more accurately the formation of receptor complexes, gels without a stacking gel system were used. As illustrated in Figures 4(c) and 4(d), only single large bands of cross-linked complexes were detected for both muscle membrane receptors. With a minigel system, electrophoresis longer than 440 V h resulted in broad and indistinctive bands; a further separation of proteins within the resolving gel could thus not be employed for the analysis of triad complexes.

After chemical reduction, re-electrophoresis of the cross-linked high-molecular-mass complex resulted in the appearance of apparent RyR and α_1-DHPR monomers (Figures 4e and 4f). Whereas immunodecoration of the reduced RyR showed only one band of approx. 565 kDa, labelling of the α_1-DHPR subjected again to electrophoresis exhibited an apparent 170 kDa monomer band, as well as higher-molecular-mass species. The broad immunodecoration of α_1-DHPR as recognized by mAb IIID5 is possibly due to incomplete reduction of complexed DHPR molecules. Alternatively, intermolecular cross-linked DHPR molecules

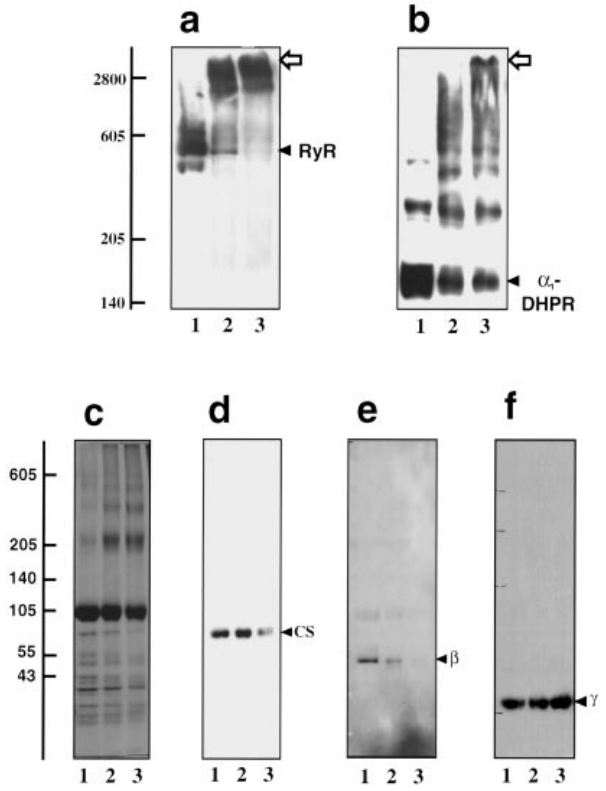

Figure 5 Cross-linking of key components of EC coupling in triads with DSP

Shown is a gel run under non-reducing conditions stained with Coomassie Blue (**c**), and identical immunoblots (**a**, **b**, **d**–**f**) of rabbit skeletal muscle triads cross-linked with DSP. Lanes 1–3 represent 0, 25 and 50 μg of cross-linker/mg of protein respectively. Immunoblots were stained with polyclonal antibodies against the C-termini of the RyR (**a**) and the β (**e**) and γ (**f**) subunits of the DHPR, as well as mAb IIID5 against the α_1-DHPR (**b**) and mAb VIIID1$_2$ against calsequestrin (CS) (**d**). Distinct overlaps of immunoreactivity for α_1-DHPR and RyR are indicated by large open arrows. Electrophoretic separation was performed on large 3–12% (w/v) (**a**, **b**) and 4–12% (w/v) (**c**–**f**) gradient gels. The positions of molecular mass standards (in kDa) are indicated at the left.

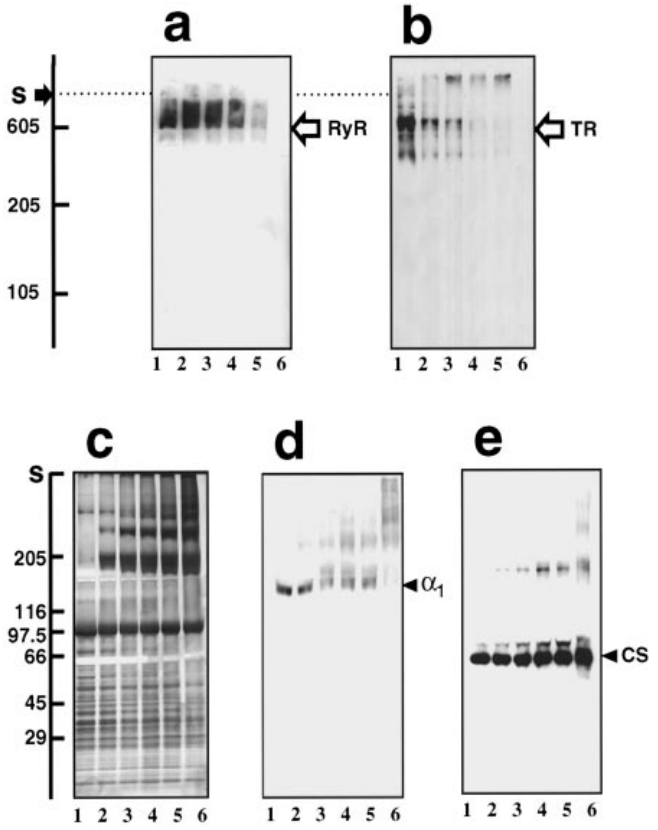

Figure 6 Cross-linking of triadin in SR with DSP

Shown is a 4–12% (w/v) gradient gel run under non-reducing conditions stained with silver (**c**), and identical immunoblots (**a**, **b**, **d**, **e**) of rabbit skeletal muscle SR cross-linked with DSP. Lanes 1–6 represent 0, 12.5, 25, 37.5, 50 and 100 μg of cross-linker/mg of protein respectively. Stacking gels are shown in (**b**) to illustrate the appearance of extremely high-molecular-mass complexes of triadin that did not enter the top of the separating gradient gel. Immunoblots were decorated with a polyclonal antibody against the C-terminus of the RyR (**a**), as well as mAb IIG12 against triadin (**b**), mAb IIID5 against α_1-DHPR (α_1) (**d**) and mAb VIIID1$_2$ against calsequestrin (CS) (**e**). In (**a**) and (**b**) the boundary between the stacking gel and the resolving gel is marked 'S'. The positions of molecular mass standards (in kDa) are indicated at the left.

and/or attachment of the α_1-DHPR to other components whose interactions are not readily reversed by chemical reduction might be responsible for these findings. Nevertheless, reduced protein bands of the 565 kDa RyR and α_1-DHPR species did not overlap as was observed before chemical reduction of the cross-linked complex (Figures 4c–4f). This demonstrates the presence of both receptor types within the high-molecular-mass band and strongly implies a complex formation between the RyR and α_1-DHPR after cross-linking.

Cross-linking analysis with large gradient gels, as shown in Figure 5, also revealed overlapping immunodecoration between the RyR and α_1-DHPR and confirmed the findings shown in Figure 4 with minigel systems. However, for these extremely large complexes, electrophoretic mobility and transfer efficiency seemed to be better with 0.75 mm thick gels with a minigel system and a minitransfer module than with thicker and larger standard gels (Figures 4 and 5). Whereas γ-DHPR exhibited broadening of its monomer band (Figure 5f), the monomers of β-DHPR and calsequestrin decreased noticeably in concentration with increasing amounts of DSP (Figures 5d and 5e). None of these components seemed to be present in the receptor complexes of more than 3000 kDa (Figures 5a and 5b), but alterations in antibody-binding sites owing to cross-linking might be responsible for the absence of detectable high-molecular-mass complexes of calsequestrin and β-DHPR. Owing to its relatively low abundance in junctional couplings, it was not possible to determine the position of high-molecular-mass clusters of triadin by using non-reducing gels.

Analysis of cross-linking with the non-reducible agent BS^3 showed a shift to a high-molecular-mass complex that was characterized by some degree of overlap of broad immunoreactive bands for the α_1-DHPR and the RyR. However, the overlap was not nearly as distinct as with DSP cross-linking, and immunodecoration was extremely weak for α_1-DHPR in the receptor complex (results not shown). In control experiments, the SR Ca^{2+}-ATPase of apparent 110 kDa showed the formation of cross-linked complexes including dimers (Figure 3g). These complexes could be electro-eluted from gel slices and could also be separated by standard two-dimensional gel electrophoresis with a non-reducing first dimension and a reducing second dimension (results not shown). However, attempts to characterize

further the cross-linked high-molecular-mass complexes between α_1-DHPR and the RyR (Figures 4 and 5), as well as extremely large complexes between the RyR and triadin (Figure 6), with the same established methods failed. Probably the relatively low abundance and/or very large size of the complex between α_1-DHPR, RyR and triadin, as evidenced by ultrastructural studies [3], complicated their elution and thus hampered the further analysis of EC-coupling complexes after cross-linking. Furthermore experiments with standard chromatography and immunoprecipitation techniques did not result in the isolation of large enough amounts of cross-linked complex for a detailed biochemical analysis (results not shown).

Immunoblot analysis of triadin in cross-linked SR

Comparative immunoblotting of SR vesicles under non-reducing conditions showed that antibody binding to disulphide-bonded clusters of triadin overlaps with immunodecoration of the RyR monomer (Figures 6a and 6b). After cross-linking, immunoreactivity for triadin was found in extremely high-molecular-mass complexes, indicative of the tendency of triadin to form clusters in the triad junction. These complexes did not enter the separating gel and must thus have molecular masses in excess of 4 MDa (Figure 6b). At 100 μg DSP/mg of protein, both triadin and the RyR were not detectable by immunoblotting (Figures 6a and 6b), indicating that these complexes are too large even to enter the 3.5% stacking gel system or are not sufficiently transferred after electrophoresis. Alternatively, cross-linking-induced conformational changes in epitopes of high-molecular-mass complexes might prevent proper antibody binding. Immunodecoration of the α_1-DHPR revealed cross-linking to high-molecular-mass complexes (Figure 6d); however, no distinct overlap with the RyR, as shown in Figures 4 and 5, could be demonstrated. Although increasing amounts of DSP resulted in a broader immunoreactive band for calsequestrin monomers and in the appearance of a second higher-molecular-mass band, no major cross-linked complexes of this SR Ca^{2+}-binding protein were observed above apparent 190 kDa (Figure 6e).

DISCUSSION

Conformational changes in the α_1-subunit of the voltage-sensing DHPR are believed to trigger Ca^{2+} release from the SR RyR directly by physical means [1–3]. To investigate the proposed direct physical contact between these two types of skeletal muscle receptors biochemically and to explore potential interactions with other muscle membrane proteins, we employed chemical cross-linking with homobifunctional probes. As alleged by many studies [29,30], chemical cross-linking techniques are an extremely powerful and unparalleled tool in studying interactions between neighbouring proteins in membranes.

Although immunoblotting of cross-linked skeletal muscle microsomes demonstrated distinct decreases in the electrophoretic mobility of most of the various EC-coupling components studied, no major complexes of triadic components were revealed. This is most probably due to the low abundance of potential triad complexes in the crude microsomal fraction. However, our immunoblot analysis of DSP-cross-linked membrane complexes in the enriched triad fraction clearly indicates a linkage between the RyR and junctional α_1-DHPR. The identification of a triad complex agrees with ultrastructural evidence, which demonstrated the existence of triadic couplings between tetrads representing the DHPR and the so-called foot region of the gigantic RyR complex [3,11]. The functional interaction between a peptide representing the cytoplasmic loop of the α_1-DHPR between repeats II and III with the RyR [12] is also in accordance with our results. In addition, the existence of a complex between the α_1-DHPR and the RyR also agrees with immunoprecipitation experiments. Antibodies to the RyR were found to co-precipitate the DHPR, whereas antibodies to the DHPR caused precipitation of the RyR [13]. Our immunoblot analysis of heavy SR vesicles, which suggests that under non-reducing conditions high-molecular-mass clusters of triadin exist in a complex with the RyR, corresponds to previous studies. Triadin seems to be of central importance for mediating between the junctional SR/transverse tubules interface by binding to various triad proteins [17–20]. Calsequestrin, which was previously proposed to be linked to triadin and the RyR [19], was not confirmed to be linked to these triad components as judged by our cross-linking results.

In contrast with our current findings, previous analyses of skeletal muscle membranes with a variety of cross-linkers [22,38] did not result in the formation of high-molecular-mass complexes between the RyR and the DHPR. It is possible that interactions between α_1-DHPR and RyR are observed only by using hydrophobic 1.2 nm cross-linkers such as DSP under the buffer and the incubation conditions described in the present study. In contrast, only a small subpopulation of cross-linkable RyR and DHPR might be available and the enrichment of these complexes in the triad fraction might be a prerequisite for the detection of these interactions. Morphological studies suggest that three different subtypes of DHPR complexes exist: an uncoupled extrajunctional complex as well as RyR-coupled and RyR-uncoupled junctional DHPR tetrads [3]. The immunodecoration of low-abundance RyR-coupled DHPR complexes might be discernible only with highly sensitive detection methods, i.e. enhanced chemiluminescence as employed in this study.

Recently Sacchetto et al. [24] reported the co-localization of the α_1-subunit of the DHPR with the Na^+/Ca^{2+} exchanger and the calmodulin-dependent Ca^{2+}-ATPase in junctional membrane domains of the transverse tubules. Because they analysed conventionally isolated subcellular fractions by density gradient centrifugation, cross-contamination between different surface membrane fractions derived from the sarcolemma and the transverse tubules cannot be excluded. Affinity-purified sarcolemma vesicles, essentially devoid of any contamination due to entrapped or associated SR or transverse-tubule vesicles, do not contain the α_1-DHPR [25]. In addition, a comparative immunoblot analysis of the main skeletal muscle membrane systems revealed that the calmodulin-dependent Ca^{2+}-ATPase, in accordance with its immunofluorescence localization, is restricted to the sarcolemma and is not present in the transverse tubule [39]. It is thus unlikely that a large subpopulation of the sarcolemmal calmodulin-dependent Ca^{2+}-ATPase is associated with the DHPR in junctional transverse tubules.

The fact that only a low-level complex formation between the α_1-DHPR and the RyR was observed agrees with more recently suggested scenarios for EC coupling in adult skeletal muscle. After an initial direct physical interaction and signal transduction between the two receptors, SR Ca^{2+} fluxes might then be amplified by a Ca^{2+}-induced Ca^{2+} release mechanism mediated by DHPR-uncoupled RyR [1–3]. Modification of interactions between RyR and DHPR might be regulated by the DHPR β-subunit or cAMP-dependent protein kinase phosphorylation of the α_1-DHPR [40]. Phosphorylation of the DHPR might shift the SR Ca^{2+} release in skeletal muscle from a more voltage-dependent to a more Ca^{2+}-dependent mechanism [1–3]. Although recent studies show that the two receptors exhibit temporal differences in their developmental induction [41] and suggest that receptor interactions are not responsible for the formation and maintenance of

junctional couplings [42], the basic hypothesis, that a close physical proximity of the α_1-DHPR to the RyR is a prerequisite for EC coupling in adult skeletal muscle fibres, remains unchallenged [1–3]. In this respect, the present study provides direct biochemical evidence for the existence of a native triad complex responsible for signal transduction by physical means in mature skeletal muscle fibres.

We thank Dr. Kevin P. Campbell (Howard Hughes Medical Institute) for a generous gift of antibodies to muscle membrane proteins. This work was supported by project grant 43987-Z-95 from the Wellcome Trust.

REFERENCES

1 Meissner, G. and Lu, X. (1995) Biosci. Rep. **15**, 399–408
2 Melzer, W., Herrmann-Frank, A. and Lüttgau, H. C. (1995) Biochim. Biophys. Acta **1241**, 59–116
3 Franzini-Armstrong, C. and Jorgensen, A. O. (1994) Annu. Rev. Physiol. **56**, 509–534
4 Catterall, W. A. (1995) Annu. Rev. Biochem. **64**, 493–532
5 Isom, L. L., DeJong, K. S. and Catterall, W. A. (1994) Neuron **12**, 1183–1194
6 Meissner, G. (1994) Annu. Rev. Physiol. **56**, 485–508
7 Brilliantes, A. B., Ondrias, K., Scott, A., Kobrinsky, E., Ondriasova, E., Moschella, M., Jayaraman, T., Landers, M., Ehrlich, B. and Marks, A. M. (1994) Cell **77**, 513–523
8 Radermacher, M., Rao, V., Grassucci, R., Frank, J., Timermann, A. P., Fleischer, S. and Wagenknecht, T. (1994) J. Cell Biol. **127**, 411–423
9 Rios, E. and Brum, G. (1987) Nature (London) **325**, 717–720
10 Adams, B. A., Tanabe, T., Mikami, A., Numa, S. and Beam, K. G. (1990) Nature (London) **346**, 569–572
11 Block, B. A., Imagawa, T., Campbell, K. P. and Franzini-Armstrong, C. (1988) J. Cell Biol. **107**, 2587–2600
12 Lu, X., Xu, L. and Meissner, G. (1994) J. Biol. Chem. **269**, 6511–6516
13 Marty, I., Robert, M., Villaz, M., DeJongh, K., Lai, L., Catterall, W. A. and Ronjat, M. (1994) Proc. Natl. Acad. Sci. U.S.A. **91**, 2270–2274
14 Flucher, B. E., Andrews, S. B. and Daniels, M. P. (1994) Mol. Biol. Cell **5**, 1105–1118
15 Yuan, S. H., Arnold, W. and Jorgensen, A. O. (1991) J. Cell Biol. **112**, 289–301
16 Flucher, B. E., Andrews, S. B., Fleischer, S., Marks, A. R., Caswell, A. and Powell, J. A. (1993) J. Cell Biol. **123**, 1161–1174
17 Kim, K. C., Caswell, A. H., Brunschwig, J. P. and Brandt, N. R. (1990) J. Memb. Biol. **113**, 221–235
18 Guo, W., Jorgensen, A. O. and Campbell, K. P. (1994) J. Biol. Chem. **269**, 28359–28365
19 Guo, W. and Campbell, K. P. (1995) J. Biol. Chem. **270**, 9027–9030
20 Fan, H., Brandt, N. R., Peng, M., Schwartz, A. and Caswell, A. H. (1995) Biochemistry **34**, 14893–14901
21 Caswell, A. H. and Corbett, A. M. (1985) J. Biol. Chem. **260**, 6892–6898
22 Brandt, N. R., Caswell, A. H., Wen, S. R. and Talvenheimo, J. A. (1990) J. Membr. Biol. **113**, 237–251
23 Thieleczek, R., Mayr, G. W. and Brandt, N. R. (1989) J. Biol. Chem. **264**, 7349–7356
24 Sacchetto, R., Margreth, A., Pelosi, M. and Carafoli, E. (1996) Eur. J. Biochem. **237**, 483–488
25 Ohlendieck, K., Ervasti, J. M., Snook, J. B. and Campbell, K. P. (1991) J. Cell Biol. **112**, 135–148
26 Sharp, A. H., Imagawa, T., Leung, A. T. and Campbell, K. P. (1987) J. Biol. Chem. **262**, 12309–12315
27 Rosemblatt, M., Hidalgo, C., Vergara, C. and Ikemoto, N. (1981) J. Biol. Chem. **256**, 8140–8148
28 Bradford, M. M. (1976) Anal. Biochem. **72**, 248–254
29 Lomant, A. G. and Fairbanks, G. (1976) J. Mol. Biol. **104**, 243–261
30 Wong, S. S. (1991) Chemistry of Protein Conjugation and Cross-linking, CRC Press, Boca Raton, FL
31 Laemmli, U. K. (1970) Nature (London) **227**, 680–685
32 Ohlendieck, K., Partin, J. S. and Lennarz, W. J. (1994) J. Cell Biol. **125**, 817–824
33 Campbell, K. P., MacLennan, D. H. and Jorgensen, A. O. (1983) J. Biol. Chem. **258**, 11267–11273
34 Etlinger, J. D., Zak, R. and Fischman, D. (1976) J. Cell Biol. **68**, 123–141
35 Harlow, E. and Lane, D. (1988) Antibodies. A Laboratory Manual, Cold Spring Harbor Laboratory, Cold Spring Harbor, NY
36 Olmsted, J. B. (1981) J. Biol. Chem. **256**, 11955–11957
37 Towbin, H., Staehelin, T. and Gordon, J. (1979) Proc. Natl. Acad. Sci. U.S.A. **76**, 4350–4354
38 Shoshan-Barmatz, V., Hadad-Halfon, N. and Ostersetzer, O. (1995) Biochim. Biophys. Acta **1237**, 151–161
39 Ohlendieck, K. (1996) Biochim. Biophys. Acta **1283**, 215–222
40 Lu, X., Xu, L. and Meissner, G. J. (1995) Biol. Chem. **270**, 18559–18464
41 Kyselovic, J., Leddy, J. J., Ray, A., Wigle, J. and Tuana, B. S. (1994) J. Biol. Chem. **269**, 21770–21777
42 Powell, J. A., Petherbridge, L. and Flucher, B. E. (1996) J. Cell Biol. **134**, 375–387

Received 9 October 1996/27 January 1997; accepted 7 February 1997